Vol. 46, No. 3 (2024) 476-485, DOI: 10.24874/ti.1609.01.24.03

Tribology in Industry

www.tribology.rs

RESEARCH

Boriding of Low-Carbon Steel by Plasma Method: Microstructure and Coating Properties

Nguyen Van Vinh[a,*], Nguyen Trung Thuy[b], Balanovskiy Andrey Evgenievich[a]

[a]*Irkutsk National Research Technical University, Russia,*
[b]*Defense Force Academy, Son Tay, Ha Noi, Viet Nam.*

Keywords:

Wear resistance
Abrasive wear
Boride iron
Plasma alloying
Boride coatings

* Corresponding author:

Nguyen Van Vinh
E-mail:
nguyenvanvinh190596@gmail.com

Received: 23 January 2024
Revised: 28 February 2024
Accepted: 15 March 2024

A B S T R A C T

In materials science, steel boration is a promising type of thermochemical diffusion process, the purpose of which is the introduction of hard and wear-resistant boride particles into the surface layers of the metal. The main disadvantage of boration is the fragility of borated layers, especially boride. Currently, there are promising methods for the formation of a composite structure, which are based on the treatment of surface layers of steels with concentrated energy flows (laser, electron beam and plasma). The work includes studies of microstructure, hardness measurements, analysis of phase composition, and determination of chemical composition in local locations, wear tests under various conditions, and adhesion testing of the coatings obtained after plasma boration. As the degree of alloying of the molten layer decreases in the direction from the surface to the base metal, zones of overeutectic, eutectic and pre-eutectic types with a different combination of structural components are formed. The material obtained after borating a mixture of 40% B + 10% Fe is characterized by the highest level of microhardness, which is 1000...1300 HV. The highest results in friction tests are provided by boration of a powder mixture of 40% B + 10% Fe.

1. INTRODUCTION

An important problem of modern materials science is to increase the strength and wear resistance of tools and various machine parts through the use of diffusion saturation of the surface of metals and alloys with various chemical elements [1]. In materials science, steel boration is a promising type of thermochemical diffusion process, the purpose of which is the introduction of hard and wear-resistant boride particles into the surface layers of the metal [1,2]. The resulting borides form extremely wear-resistant zones, consisting mainly of Fe2B [2]. In industrial practice, the following main types of boration of parts are used: liquid electrolysis, non-electrolysis liquid, gas, powder [2]. Liquid boration treatment is carried out in a borax melt; 30-40% boron carbide is also added to the composition. Unlike electrolysis boration, the final result is not determined by the shape of the workpiece. The main disadvantage of the

method is that the working melt is rapidly depleted, which limits the use of the described method [3,4]. Modern processes of chemical and thermal boration treatment are often carried out using powders containing boron carbide with the addition of ammonium chloride, which reduces the cost of the process and allows you to do without special equipment [4]. Powder boration is particularly suitable for non-alloy and low-alloy steels. With an increase in the content of alloying elements, the diffusion rate and, consequently, the thickness of the achievable boride layer decreases [5]. The process is labor-intensive; therefore it is mainly used in mass industrial production [5,6]. Gas boration is characterized by increased activity of thermodiffusion processes. Therefore, it can be used at lower temperatures (from 600 °C). The disadvantage of the method is the increased explosion hazard and toxicity of the gas mixtures used [7,8]. It should be noted that solid-phase methods of carrying out these methods of chemical heat treatment require prolonged exposure at high temperatures, which negatively affects the structure and properties of the base material. Boration usually leads to the formation of a needle-like microstructure of FeB and Fe2B. The main disadvantage of boration is the fragility of borated layers, especially boride [8].

Currently, there are promising methods for the formation of a composite structure, which are based on the treatment of surface layers of steels with concentrated energy flows (laser, electron beam and plasma) [9-11]. Surface alloying methods associated with the effects of laser radiation, high-power electron beams, and plasma fluxes on materials allow local processing of those areas of parts that are subjected to the most intense wear and contact fatigue loading. In addition, the use of concentrated heating sources makes it possible to increase the depth of the hardened layer [10,11]. High heating and cooling rates, implemented using high-energy methods, can significantly reduce the processing time [12]. Cheng et al. used the so called preplaced powder method, applying the laser treatment on CrB2 powder, pasted as a slurry on the surface of stainless steel [13]. Other investigators used TiB2 on the surface of plain and tool steels by pressing or pasting the powder and then melting it by using electron beam [14]. TiB2 was also applied on plain and tool steels with a paint spray gun and the precursor powder melted using laser alloying techniques [15]. Other scientists used the so called powder injection method, feeding CrB [16] or CrB2 [17,18] powders directly in the laser beam, in order to alloy the surface of plain steels and improve their wear characteristics. The increase of borided layer plasticity on the steel surface was successfully reached in [19] by means of this surface coating electron beam irradiation. The study [20] has shown that boride coatings on low carbon steel can be developed effectively and economically using manufactured SMAW electrodes. Kim et al. used PTA to produce highly alloyed deposits with Armacor powders (chromium–boron rich commercial powders characterised as metamorphic) and examined their microstructure and wear properties [21].

The aim of this paper is to investigate the boriding process of plain steel using the plasma transferred arc alloying technique. The work includes studies of microstructure, hardness measurements, analysis of phase composition, and determination of chemical composition in local locations, wear tests under various conditions, and adhesion testing of the coatings obtained.

2. PROCEDURES–EXPERIMENTAL TECHNIQUES

2.1 Materials

AISI 1018 steel samples with a size of 75×15×15 mm were used as a substrate. The choice of this steel is due to the wide distribution of ferrite-pearlitic steels for the manufacture of machine parts and structural elements, its low cost, as well as the use of various types of chemical-thermal treatment in order to increase wear resistance. Its microstructure is shown in Fig. 1. Amorphous boron powders were used to form hardened coating layers on the steel surface. The average particle size of the powder is 5-20 microns. An adhesive based on the BF-2 standard was used as a binder. Preparation of the coating before processing was carried out as follows. The powders were mixed with BF-2 glue with a ratio of 1:1 to obtain a mixture with good viscosity. The suspension was applied to the surface of the samples, and then heated to dry at 60 ° C for 2 hours before plasma treatment. The plasma doping scheme and processing parameters are shown in Fig. 2 and Tab. 1.

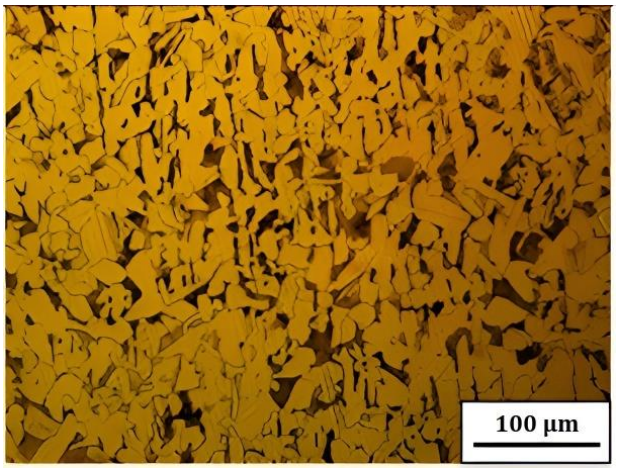

Fig. 1. The structure of steel 20 before processing.

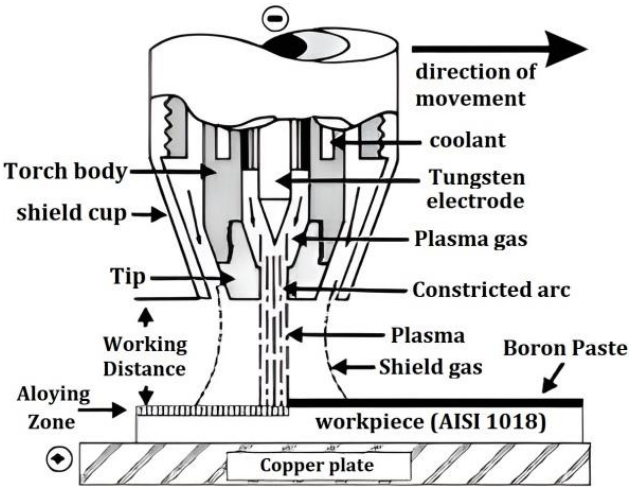

Fig. 2. Plasma alloying scheme.

Table 1. Parameters of the plasma alloying process.

№ sample	The composition of the mixture % by weight			Current [A]	Scanning speed [mm/s]
	Fe	B	BF2		
1	10	40	50	140	4
2	25	25	50		
3	40	10	50		

The microstructure of boride coatings was studied using an optical microscope MET-2 and a double-beam scanning microscope JIB-4500. The boron content of the doped coating is determined by the method of an electron probe microanalyzer. The phase composition of the coatings after plasma alloying was analyzed using a Shimadzu XRD-7000 X-ray diffractometer using Cu-Kα radiation. The samples were scanned in step-by-step scanning mode in the range of 5°-85° in 5° increments at 40 kV and 40 mA. The microhardness of the doped layer was measured using a SHIMADZU HMV-2 microhardness meter with a load of 0.98 N.

2.2 Assessment of the wear resistance of the studied materials under the influence of fixed abrasive particles

The assessment of the wear resistance of the studied materials under the influence of fixed abrasive particles was carried out according to the scheme shown in Fig. 4. During the tests, a 10x5x10 mm sample was statically pressed against an abrasive cloth mounted on a rotating disk. The load is 50 N. At the same time, the working surface of the studied samples was in full contact with an abrasive cloth with a grain size of 80. The grains were silicon carbides. During the friction process, the sample made a translational movement in the radial direction from the center to the periphery. A sample of cemented steel was used as a reference, the wear resistance of which was taken as a unit.

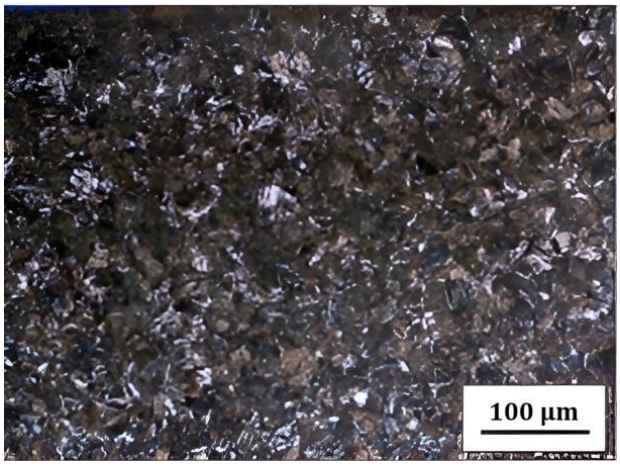

Fig. 3. Microstructure of cemented steel 20.

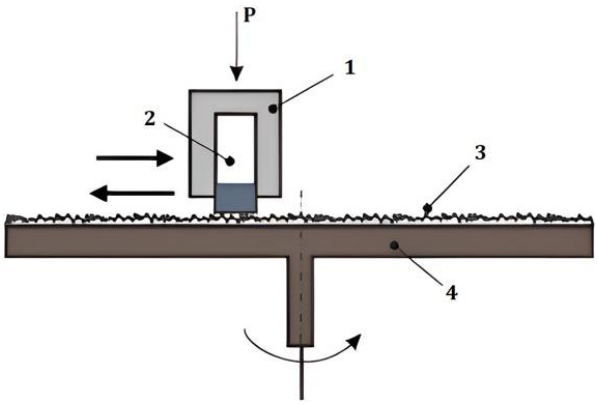

Fig. 4. Friction test scheme under the influence of fixed abrasive particles: 1 – holder; 2 – sample; 3 – abrasive cloth; 4 – aluminum disc.

Diffusion saturation of steel 20 with carbon during furnace heating was carried out in the medium of a charcoal carburetor. The duration

of the saturation process was 4 hours, and the temperature was 1100 ° C. After chemical and thermal treatment, the samples were subjected to quenching (850 ° C) and low tempering (250 ° C) for 2 hours. After cementation, the hardness of the carbonized layer is 60-64 HRC. Prior to the tests, samples were processed to achieve a complete fit of the samples to the abrasive disc and a roughness of the working surface Ra ≈ 0.32 μm.

To assess the wear resistance of the materials under study, the weight loss of the samples was determined by the test time. Weighing is carried out using analytical scales. At least 3 samples were tested for friction of each material. The relative wear resistance of materials was calculated by the formula (GOST 6556-82):

$$\varepsilon = \frac{\Delta m_1}{\Delta m_0} \times \frac{\rho_0}{\rho_1}$$

Where: ρ_0, ρ_1 – the density of the studied and reference materials; Δm_0, Δm_1 – the amount of mass loss of the reference and test samples.

2.3 The wear resistance of the coatings was evaluated under sliding friction conditions according to the "block by ring" scheme

The test scheme is shown in Figure 5. The tests were carried out in accordance with the international standard ASTM G-77. When the disc rotates at a frequency of 400 rpm, the test sample wears out. The test samples are cut out in the form of a 12x5x10 mm plate. A disk made of hardened steel grade 45 with an outer diameter of 40 mm and a width of 10 mm was used as an indenter. we used heat-treated grade 45 steel. The steel hardening process consists of heating grade 45 steel to a temperature of 830-850 °C and cooling at a certain speed in water. After heat treatment, the steel has a hardness of 45...50 HRC. During the test, the samples were pressed against the indenter with a constant load of 300 N. During the testing of each sample, the friction path was 10,800 m. At the end of the tests, measurements of the size of the wear hole were carried out. After the test, the wear marks were measured using an optical microscope and a profilometer to determine the degree of wear. The wear rate is defined as the total loss of material volume in m³ divided by the total sliding distance in meters.

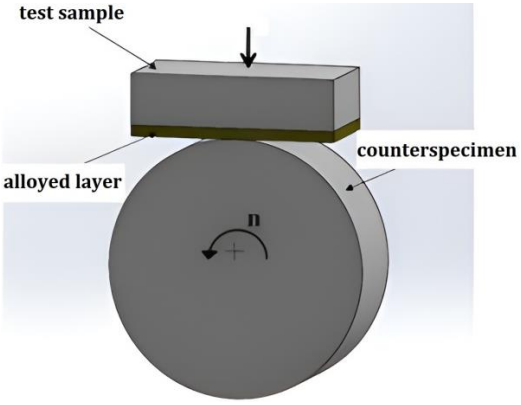

Fig. 5. The scheme of testing samples under sliding friction conditions.

The wear resistance of the deposited layers was estimated based on the volume of worn material, which was calculated based on the results of measurements of the geometry of the wear hole using a Brinell magnifier.

$$V = \frac{R^2}{2}\left(arrcos\left(1-\frac{l^2}{2R^2}\right) - \sqrt{1-\left(1-\frac{l^2}{2R^2}\right)^2}\right) \times d$$

where R – the radius of the counterbody, mm; l – the length of the hole, mm; d – the thickness of the abrasion disc (counterbody), mm.

2.4 Rockwell-C adhesion test

The Rockwell-C adhesion test results in damage to the layer adjacent to the dent boundary. The type and volume of the fracture zone of the coating show the adhesion of the layer and its fragility. The indenter causes extreme shear stresses at the interface. Coatings with good adhesion are able to withstand these shear stresses and prevent long-term peeling around the circumference from the dent. Moreover, extensive exfoliation near the dent indicates poor interfacial adhesion. After indentation, an optical microscope was used to evaluate the test. The HF1–HF4 species determine sufficient adhesion, whereas HF5 and HF6 represent insufficient adhesion.

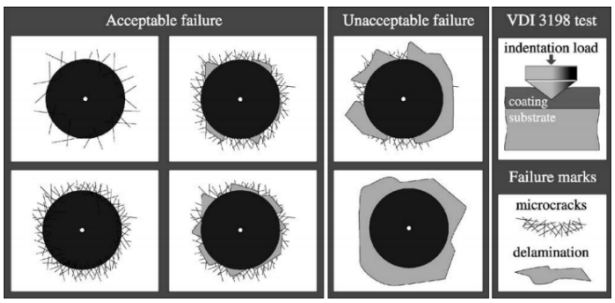

Fig. 6. The adhesion quality control [22].

3. RESULTS AND DISCUSSION

3.1 Microstructure and hardness

Figure 7 shows the microstructure of sample 10Fe-40B after plasma doping with boron.

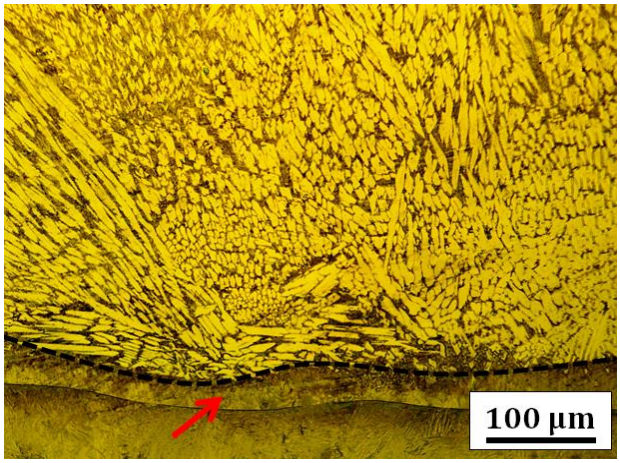

Fig. 7. Microstructure of sample 10Fe-40B after plasma alloying.

It is noted that the doped layer is characterized by a pronounced heterogeneous structure. This can be explained by the intensive mixing of alloying elements with the base material due to convection and vortex movements under the influence of plasma flow. In addition, the high rate of heating and cooling (до 200…300 °C/c) during plasma processing also explains the production of such a microstructure in steel. Metallographic analysis methods have established that accumulations of borides arbitrarily oriented in solid solution are observed in the doped layer. The morphology of borides varies from rounded to columnar. In addition, it was noted that the boundary between the alloyed layer and the base metal is clearly revealed in the form of a thin strip indicated in Fig. 7 by a red arrow. There are no defects in the form of detachments. According to the results of X-ray phase analysis (Fig. 8), the main phases released in deposited layers of this type are α-Fe, iron boride Fe2B and FeB.

Figure 9 shows the microstructure of sample 2 after boration. It can be seen that the alloyed layers of both samples 10Fe-40B and 25Fe-25B consist of several characteristic zones (the boundaries between the zones are indicated by dashed lines) (Fig. 7 and 9). The formation of a transeutectic type structure has been recorded in the surface layers, which is characterized by the separation of primary crystals of boride phases of various morphologies distributed in the eutectic matrix. With further progress to the base metal, the concentration of boron is not enough to isolate borides, so the structure of the layer is represented only by colonies of eutectic. According to the results of X-ray phase analysis (Fig. 10), the main phases released in deposited layers of this type are α-Fe, iron boride Fe2B and FeB.

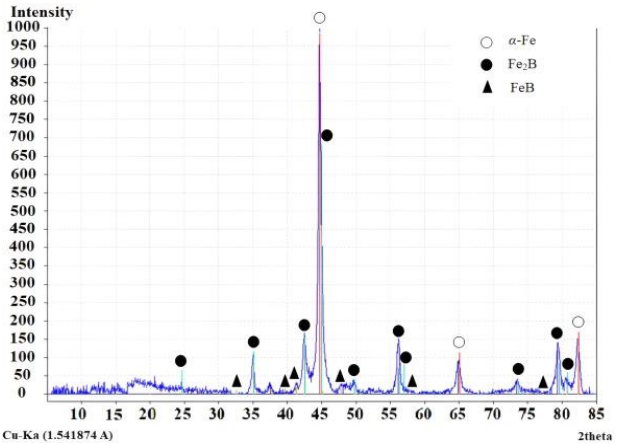

Fig. 8. X-ray images of sample 10Fe-40B after plasma alloying

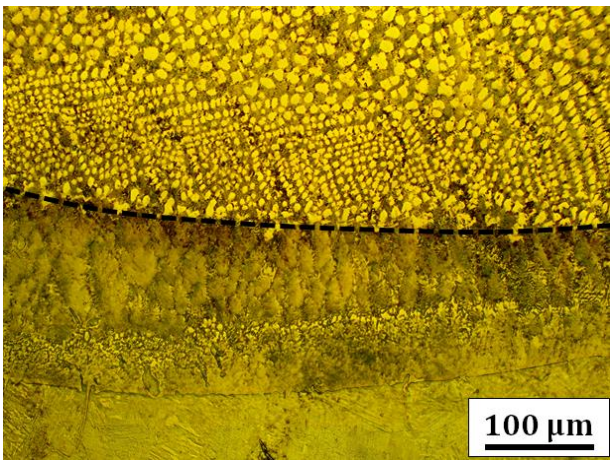

Fig. 9. Microstructure of sample 25Fe-25B after plasma alloying.

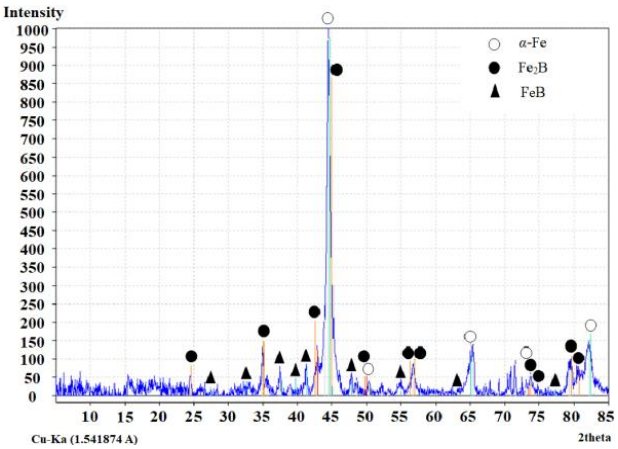

Fig. 10. X-ray images of sample 25Fe-25B after plasma alloying.

In the course of microstructure studies, it was found that colonies of a mechanical mixture of a lamellar type are isolated in micro volumes between boride crystals (Fig. 11). The eutectic structure is formed as a result of simultaneous crystallization of alpha-iron and boride phases at a certain temperature. Eutectic components are characterized by different structure, dispersion, as well as quantitative ratios between phases. In addition, the formation of eutectic colonies in the form of localized areas, located, as a rule, near the boundaries with the base metal, has been recorded (Fig. 12).

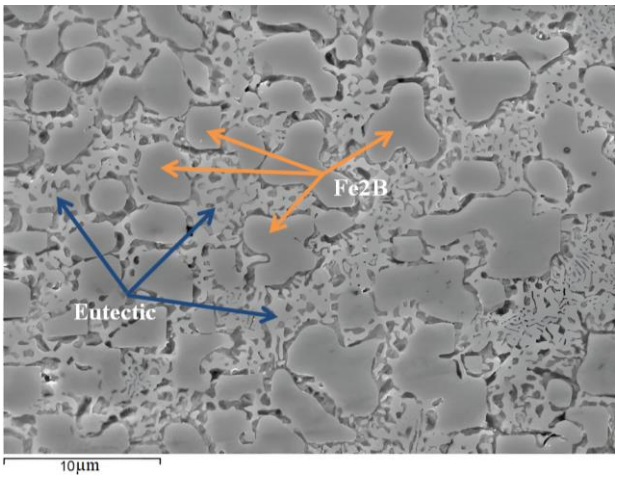

Fig. 11. Structural features of the surface layer of sample 25Fe-25B after formation (SEM).

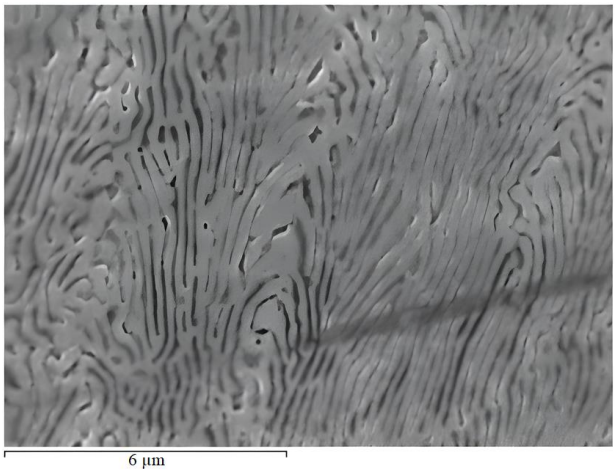

Fig. 12. Eutectic colonies of sample 25Fe-25B.

Figure 13 shows the microstructure of sample 40Fe-10B after boration. It is noted that the structure of the doped layer has a pre-eutectic type. Primary dendrites of α-solid boron solution in iron are isolated in the doped layer (Fig. 15), around which a rim of boride eutectic is formed. The eutectic consists of Fe2B and α-Fe. Primary crystals of Fe2B iron borides have not been fixed, which is explained by the relatively low concentration of boron in the molten metal. The presence of reflexes of this phase on the X-ray (Fig. 14) is probably due to its presence in the composition of the eutectic.

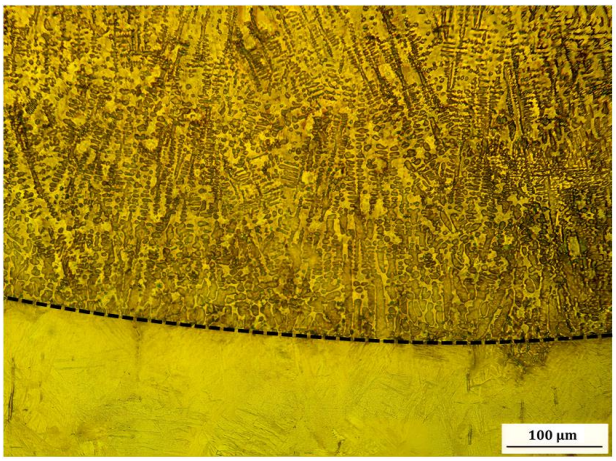

Fig. 13. Microstructure of sample 40Fe-10B after plasma alloying.

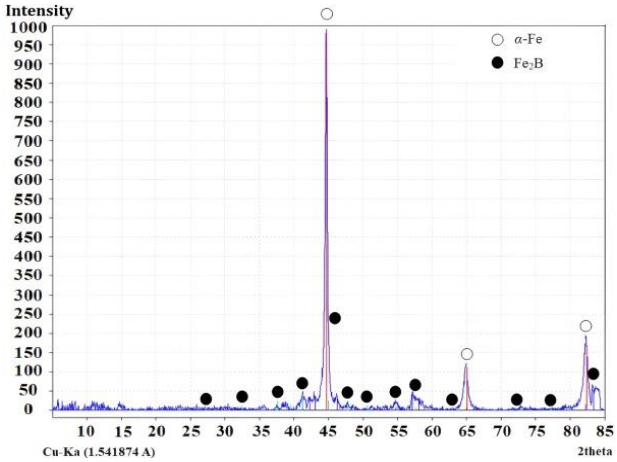

Fig. 14. X-ray images of sample 40Fe-10B after plasma alloying.

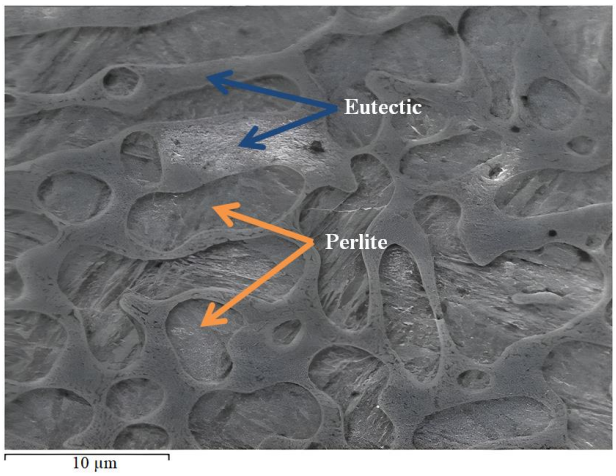

Fig. 15. Feature of the structure of the doped layer of the sample 40Fe-10B.

In Fig. 16 shows the distribution of microhardness of alloyed layers after boriding. It has been experimentally established that the highest level of microhardness is characteristic of the borated layer obtained by boriding using a powder mixture of 10% Fe + 40% B + 50% BF-2, and amounts to 1000...1300 HV.

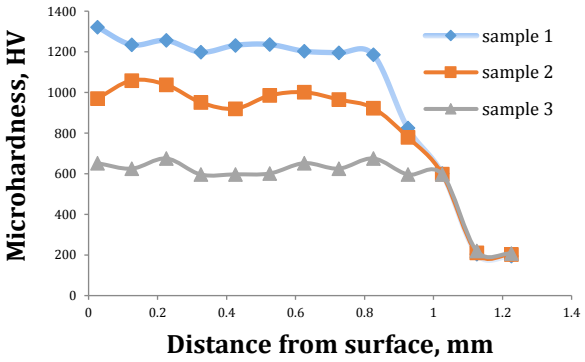

Fig. 16. Microhardness distribution of alloyed layers after boration.

The microhardness values of the alloyed layer of sample 25Fe-25B and sample 40Fe-10B are 800...1050 HV and 550...650 HV. It can be seen that the degree of hardening is determined by the volume fraction of the high-strength phase, which are iron boride particles. A decrease in the boron content leads to a change in the structure and a decrease in the volume fraction of primary borides, therefore, leads to a decrease in the microhardness of the alloyed layer.

3.2 Wear resistance of surface layers under friction under the influence of fixed abrasive particles

Figure 17 shows the results of tests for wear resistance against friction against fixed abrasive particles of coatings obtained using boron plasma alloying technology. As a reference, samples were made of steel 20 subjected to cementation. The wear resistance of these samples was taken as a unit.

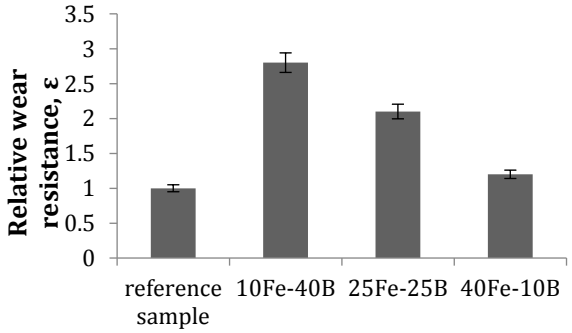

Fig. 17. Relative wear resistance of coatings after boration.

It can be seen that the best results were shown by the materials obtained during treatment using a powder mixture of 40 % B + 10 % Fe. In comparison with the samples obtained by cementation technology, an approximately three-fold increase in the resistance of the alloy was recorded. The forming frame of highly durable particles (iron borides) prevents the removal of material as a result of the introduction of abrasive particles. The relationship between the increased resistance characteristics under conditions of abrasive wear and the microhardness level of the hardened layers has been established. Boration of steel from a powder mixture of 25% B + 25 % Fe leads to the formation of surface layers, the abrasive resistance of which is 2 times higher compared to the control sample. It is noted that a decrease in boron content leads to an increase in the intensity of wear. In the structure of the coating layers of sample 40Fe-10B, the volume fraction of high-strength particles decreases, while the hardness of the eutectic matrix is insufficient to effectively resist the effects of abrasive. The wear resistance of such a coating is close to the control material.

3.3 Wear resistance of surface layers under sliding friction conditions

Figure 18 shows the volumetric wear of materials under sliding friction conditions. The results showed that the coating from a powder mixture of 40% B + 10% Fe has the best wear resistance index. The volume wear is 0.015 m^3. The presence of a large number of deep furrows is not recorded on the friction surface of such a material; however, the staining of the material is clearly observed (Fig. 19). The wear volume of the coating layers obtained after boration using a powder mixture of 25% Fe + 25% B is slightly less and amounts to 0.0185 mm^3. Wide furrows are also observed on the friction surface of these samples.

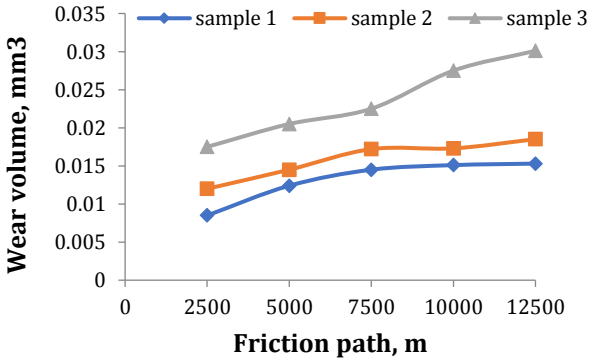

Fig. 18. Volumetric wear of materials under conditions of sliding friction.

The process of wear of the coating of sample 40Fe-10B occurs more intensively and leads to a loss of 0.03 mm^3 of material. A large number of wide furrows are observed on the wear surface of the sample, indicating a high intensity of the fracture process (Fig. 19c). During the tests under sliding friction conditions, the nature of the change in the coefficient of friction was evaluated depending on the boron content in the powder mixture. It is established that the coefficient of friction of the studied materials does not change significantly and is 0.08...0.09.

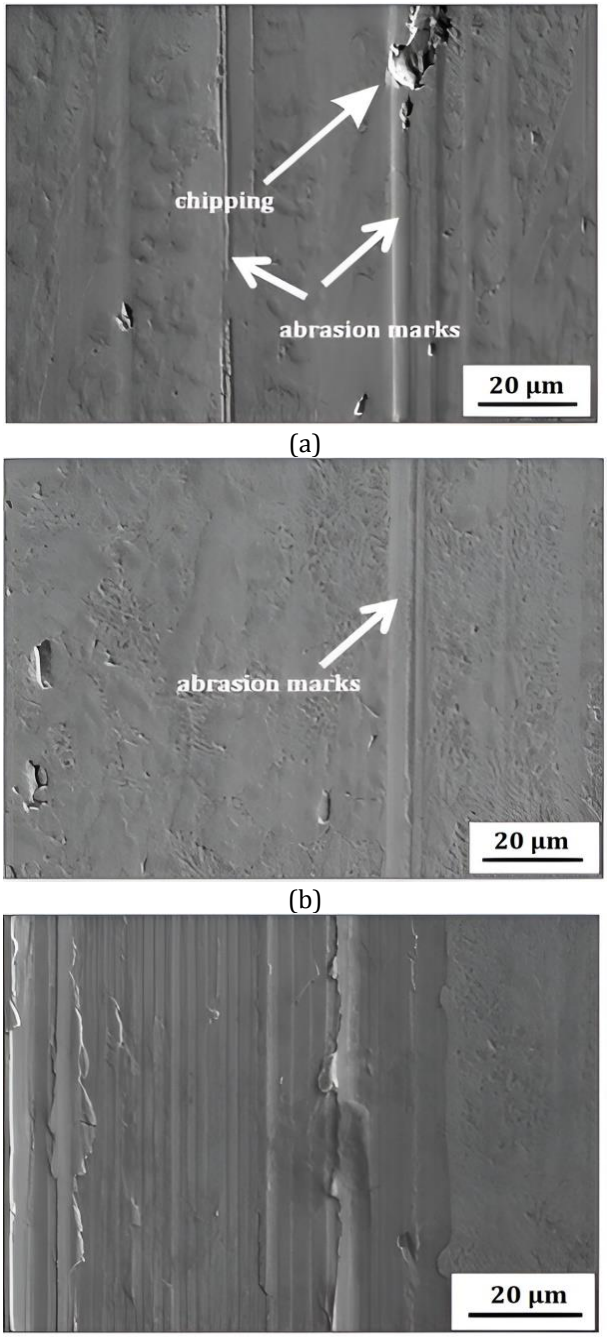

Fig. 19. Wear surfaces of deposited layers after friction (a) spalling; (b) scratches; (c) wide furrows.

3.4. Adhesion test

The Rockwell-C adhesion test results in damage to the layer adjacent to the dent boundary. The type and volume of the fracture zone of the coating show the adhesion of the layer and its fragility.

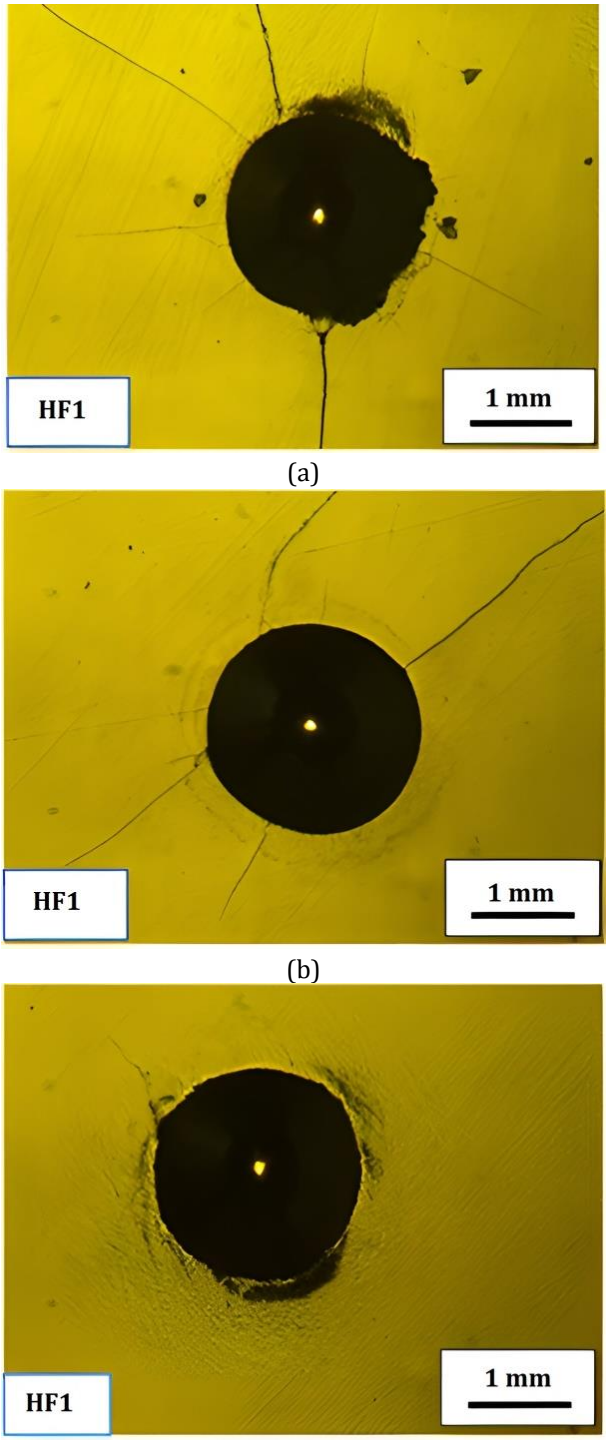

Fig. 20. Adhesion test of coatings after boration: (a) coating of sample 10Fe-40B; (b) coating of sample 25Fe-25B; (c) coating of sample 40Fe-10B.

Figure 20 shows the results of the Rockwell-C adhesion test. A conical diamond tip with an angle with a rounded top of 120 degrees. The load on the indenter is 1471 N. Compared with the control quality (Fig. 6) the coatings after boration have the HF1 quality. It is noted that coatings with good adhesion are able to withstand these shear stresses and prevent prolonged peeling around the circumference from the dent.

4. CONCLUSIONS

Based on the conducted research, it is possible to make the following conclusions:

1. Surface alloying of low–carbon steel using plasma boration technology using mixtures of "amorphous boron - iron" contributes to the production of boride coatings. A decrease in the boron content in the powder mixture leads to a decrease in the volume fraction of primary iron borides in the structure of the coating layers.
2. The treatment of powder mixtures with high-energy plasma beams leads to the formation of a gradient heterophase structure of alloys, the main type of hardening phase of which are iron borides. As the degree of alloying of the molten layer decreases in the direction from the surface to the base metal, zones of overeutectic, eutectic and pre-eutectic types with a different combination of structural components are formed.
3. The material obtained after borating a mixture of 40% B + 10% Fe is characterized by the highest level of microhardness, which is 1000...1300 HV. A decrease in the volume fraction of iron borides in the structure of the alloyed layers is accompanied by a decrease in the microhardness of the alloy to 550...650 HV.
4. The highest results in friction tests under the action of fixed abrasive particles are provided by boration of a powder mixture of 40% B + 10% Fe. The wear resistance of the material obtained according to the indicated regime is almost 3 times higher compared to low-carbon cemented steel.
5. The material obtained by borating a powder mixture of 40% B + 10% Fe has the maximum resistance during sliding friction tests on the "block ring".
6. According to the results of the adhesion test, the coatings have the quality of HF1, that is, coatings with good adhesion are able to withstand these shear stresses and prevent prolonged peeling around the circumference from the dent.

ORCID iDs

Nguyen Van Vinh 0000-0001-6514-9015
Nguyen Trung Thuy 0000-0002-5876-9256
Balanovskiy A. Evgenievich 0000-0002-6466-6587

REFERENCES

[1] T. W. Spence and M. M. Makhlouf, “Characterization of the operative mechanism in potassium fluoborate activated pack boriding of steels,” *Journal of Materials Processing Technology*, vol. 168, no. 1, pp. 127–136, Sep. 2005, doi: 10.1016/j.jmatprotec.2004.10.015.

[2] I. Campos-Silva, M. Ortíz-Domínguez, J. Martínez-Trinidad, N. López-Perrusquia, E. Hernández-Sánchez, “Properties and Characterization of Hard Coatings Obtained by Boriding: An Overview,” *Defect and Diffusion Forum*, vol. 297–301, pp. 1284–1289, Apr. 2010, doi: 10.4028/www.scientific.net/ddf.297301.1284.

[3] G. Kartal, S. Timur, C. Arslan, “Effects of process current density and temperature on electrochemical boriding of steel in molten salts,” *Journal of Electronic Materials*, vol. 34, pp. 1538–1542, Dec. 2005, doi: 10.1007/s11664-005-0162-x.

[4] V. Sista, O. Kahvecioglu, G. Kartal, Q.Z. Zeng, J.H. Kim, O.L. Eryilmaz, A. Erdemir, “Evaluation of Electrochemical Boriding of Inconel 600,” *Surface and Coatings Technology*, vol. 215, pp. 452–459, Jan. 2013, doi: 10.1016/j.surfcoat.2012.08.083.

[5] Y. Wu, Y. Lu, Y. Duan, X. Zhou, M. Peng, X. Wang, S. Zheng, “Microstructure and wear properties of powder-pack borided Ti–5Al–2.5Sn alloy,” *Journal of Materials Research and Technology*, vol. 23, pp. 4032-4043, Mar.-Apr. 2023, doi: 10.1016/j.jmrt.2023.02.052.

[6] Y. Wu, X. Zhou, X. Wang, Y. Lu, M. Peng, Y. Duan, “Microstructure and Some Properties of Powder-pack Borided Ti–5Mo–5V–8Cr–3Al Alloy With Special Attention to the Microstructure at the Interface TiB/Substrate,” *Ceramics International*, vol. 48, no. 17, pp. 24346–24354, Sep. 2022, doi: 10.1016/j.ceramint.2022.04.347.

[7] N. Makuch, "Influence of nickel silicides presence on hardness, elastic modulus and fracture toughness of gas-borided layer produced on Nisil-alloy," *Transactions of Nonferrous Metals Society of China*, vol. 31, iss. 3, pp. 764-778, Mar. 2021, doi: 10.1016/S1003-6326(21)65537-1.

[8] N. Makuch, M. Kulka, "Fracture Toughness of Hard Ceramic Phases Produced on Nimonic 80A-alloy by Gas Boriding," *Ceramics International*, vol. 42, no. 2, pp. 3275–3289, Feb. 2016, doi: 10.1016/j.ceramint.2015.10.119.

[9] Taheri Peyman, "Nanocrystalline Structure Produced by Complex Surface Treatments: Plasma Electrolytic Nitrocarburizing, Boronitriding, Borocarburizing, and Borocarbonitriding," *Plasma Processes and Polymers*, vol. 4, no. S1, pp. S721–S727, May 2007, doi: 10.1002/ppap.200731805.

[10] P. Gopalakrishnan, P. Shankar, R.V. Subba Rao, M. Sundar, S.S. Ramakrishnan, "Laser Surface Modification of Low Carbon Borided Steels," *Scripta Materialia*, vol. 44, no. 5, pp. 707–712, Mar. 2001, doi: 10.1016/s1359-6462(00)00674-6.

[11] M. Iqbal, I. Shaukat, A. Mahmood, K. Abbas, M.A. Haq, "Surface Modification of Mild Steel With Boron Carbide Reinforcement by Electron Beam Melting," *Vacuum*, vol. 85, no. 1, pp. 45–47, Jul. 2010, doi: 10.1016/j.vacuum.2010.03.009.

[12] I. A. Bataev, A. A. Bataev, M. G. Golkovsky, A. Yu. Teplykh, V. G. Burov, S. V. Veselov, "Non-vacuum Electron-beam Boriding of Low-carbon Steel," *Surface and Coatings Technology*, vol. 207, pp. 245–253, Aug. 2012, doi: 10.1016/j.surfcoat.2012.06.081.

[13] F.T Cheng, C.T Kwok, H.C Man, "Laser Surfacing of S31603 Stainless Steel With Engineering Ceramics for Cavitation Erosion Resistance," *Surface and Coatings Technology*, vol. 139, no. 1, pp. 14–24, May 2001, doi: 10.1016/s0257-8972(00)01103-8.

[14] K. Euh, S. Lee, K. Shin, "Microstructure of TiB2/Carbon Steel Surface-alloyed Materials Fabricated by High-energy Electron Beam Irradiation," *Metallurgical and Materials Transactions A*, vol. 30, no. 12, pp. 3143–3151, Dec. 1999, doi: 10.1007/s11661-999-0225-3.

[15] A. Arvind, N. B. Dahotre, "Comparative Wear in Titanium Diboride Coatings on Steel Using High Energy Density Processes," *Wear*, vol. 240, no. 1–2, pp. 144–151, May 2000, doi: 10.1016/s0043-1648(00)00357-4.

[16] A. Glozman, M. Bamberger, "Phase Transitions and Microstructure of a Laser-induced Steel Surface Alloying," *Metallurgical and Materials Transactions A*, vol. 28, no. 8, pp. 1699–1703, Aug. 1997, doi: 10.1007/s11661-997-0261-9.

[17] G. Shafirstien, "Laser Surface Alloying of Carbon Steel and α-Fe With CrB2," *Surface and Coatings Technology*, vol. 45, no. 1–3, pp. 417–423, May May 1991, doi: 10.1016/0257-8972(91)90251-q.

[18] S. Klachuk, M. Bamberger, "Laser surface alloying of 1045 AISI steel using Ni–CrB2 powder," *Materials Science and Technology*, vol. 26, no. 9, pp. 1059–1067, Sep. 2010, doi: 10.1179/026708309X12459430509337.

[19] A. A. Novakova, I. G. Sizov, D. S. Golubok, T. Yu. Kiseleva, P. O. Revokatov, "Electron-beam Boriding of Low-carbon Steel," *Journal of Alloys and Compounds*, vol. 383, no. 1–2, pp. 108–12, Nov. 2004, doi: 10.1016/j.jallcom.2004.04.017.

[20] M. Eroglu, "Boride Coatings on Steel Using Shielded Metal Arc Welding Electrode: Microstructure and Hardness," *Surface and Coatings Technology*, vol. 203, no. 16, pp. 2229–2235, May 2009, doi: 10.1016/j.surfcoat.2009.02.010.

[21] K. Hyung-Jun, G. Stephanie, K. Young-Gak, "Wear Performance of Metamorphic Alloy Coatings," *Wear*, vol. 232, no. 1, pp. 51–60, Sep. 1999, doi: 10.1016/s0043-1648(99)00160-x.

[22] D. Arslan, R. O. Uzun, "Adhesive Behavior of the Pack-Borided AISI 304L Steel With Microwave Hybrid Heating," *Celal Bayar University Journal of Science*, vol. 17, no. 2, pp. 181–191, Jun. 2021, doi: 10.18466/cbayarfbe.826118.